

Simultaneous TG-DTA Study of Cellulose Ethers in Flame Retardant Formulations

Viju Kumar V.G.

Department of Chemistry, University College, Trivandrum, Kerala - 695034, India
vgviju@gmail.com

Available online at: www.isca.in, www.isca.me

Received 30th April 2016, revised 29th May 2016, accepted 1st July 2016

Abstract

Cellulose ethers have very good compatibility and solubility characteristics and are useful for research community and industry. The present investigation purports the application of proven flame retardant formulations on cellulose ethers such as methylcellulose, ethylcellulose, hydroxyethylcellulose, carboxymethylcellulose sodium salt and hydroxypropylmethylcellulose. Binary formulations of cellulose ethers with inorganic additives like zinc(II) chloride, cadmium (II) bromide, boric acid, borax, diammonium hydrogenphosphate, sodium dihydrogenphosphate and ammonium nickel (II) sulphate were prepared. The simultaneous TG, DTG, and DTA curves were recorded in dynamic air. The phenomenological and kinetic aspects of thermal decomposition are studied in detail. The thermal behavior of binary systems is explained based on increased char and decreased volatile formation. Cellulose ethers show two-stage decomposition and the DTG peaks can be shifted using appropriate additives. To assess the thermal characteristics in a quantitative manner, the kinetic parameters such as order parameter, energy of activation, pre-exponential factor and entropy of activation for the decomposition stages have been determined using Coats-Redfern equation. The mechanism of thermal decomposition stages has also been elucidated, and most of the reactions follow random nucleation with one nucleus on each particle.

Keywords: Cellulose ethers, Thermogravimetry, Flame retardant materials, Decomposition kinetics, Coats-Redfern equation.

Introduction

Cellulose ethers have very good compatibility and solubility characteristics and are useful particularly for coating purposes and in pharmaceutical, textile, construction engineering and paper industry¹. The nonionic cellulose ethers have been found suitable for use with synthetic fibers.

The structure of cellulose ethers are responsible for its good solvency, low melting temperature, liquid crystallinity and excellent processability. Due to its various synthetic applications, cellulose ethers may encounter elevated temperatures and the presence of various ions. The literature survey gave plenty of citations about the effect of flame retardant additives in the thermal decomposition kinetics of cellulose but a few are found for cellulose ethers. Thermal decomposition kinetics of methylcellulose and ethyl cellulose in nitrogen and air by thermogravimetry has been already reported² but no extensive study on its flame retardant formulations.

In this scenario, the investigation purports the application of proven flame retardant formulations on the some important cellulose ethers. The present work aims to use simple kinetic model resulting from global mass loss from experiments of dynamic mass loss carried out and, contrary to most of the researchers who have restricted their investigations to a single series of additives.

Materials and Methods

The cellulose ethers such as methylcellulose (MC), ethylcellulose (EC), hydroxyethylcellulose (HEC), hydroxypropylmethylcellulose (HPMC) and carboxymethylcellulose sodium salt (CMC) are selected for the present investigation. For MC (soluble in cold water) methoxy substitution is 26 - 32%. The viscosity of 2% aqueous solution is 300 - 500 cps. The sulphate ash is 1.0%. For EC, the degree of substitution is 2.42 - 2.53. The viscosity of 5% w/w solution in 80:20 toluene:ethanol by weight at 25°C is 14cps. HPMC, the methoxy content is 28.6% and hydroxypropyl content is 7.3%. It shows an apparent viscosity of 13.6 cps. Loss of drying at 100°C is 3.7%. For HEC, the 1% aqueous solution shows a viscosity of 145 millipoise with a hydroxyethyl content of 13.5%. The samples were purchased from Aldrich. Sodium salt of CMC was purchased from Merck shows a loss of drying $\leq 10\%$ at 110°C. The viscosity of 1% aqueous solution at 20°C is 1100 - 1900 cps and the assay (Na; on dried substance) 6.5 - 10.8% and the sulphated ash 20 - 33.3%.

For impregnation, seven inorganic substances such as zinc (II) chloride, cadmium (II) bromide, boric acid, borax, diammonium hydrogenphosphate (AHP), sodium dihydrogenphosphate (SHP) and ammonium nickel (II) sulphate (ANS) were used as flame retardant (FR) additives. The additive impregnated samples from 5% (w/w) solid solutions. The prepared samples were pre heated to 50°C for one hour, thoroughly powdered and kept in

vacuum desiccators. The simultaneous TG, DTG, and DTA curves for forty samples were recorded using Mettler Toledo STARE thermal analysis system. A linear heating rate of $10^{\circ}\text{C min}^{-1}$ in an atmosphere of dynamic air (flow rate, $\sim 60 \text{ mL min}^{-1}$) with a sample mass of $\sim 3 \text{ mg}$ were used for all the TG measurements in the temperature range of ambient to $\sim 700^{\circ}\text{C}$. The kinetics of decomposition has been studied using the Coats-Redfern equation³. The phenomenological and kinetic aspects of thermal decomposition of these samples are studied in detail. To assess the thermal characteristics in a quantitative manner, the kinetic parameters such as order parameter (n), energy of activation (E), pre-exponential factor (A) and entropy of activation (ΔS) for the decomposition stages of the materials have been determined. For the determination of mechanism of reaction using non-isothermal method, the equations proposed by Satava are employed⁴.

Results and Discussion

The metal ions have a pronounced effect on the decomposition of cellulose and its derivatives, reduce combustibility of the products, and retard flame spread. The TG and DTA data for cellulose ethers and additive impregnated samples show that the introduction of metal ions in the form of inorganic salts result in i. a decrease in the temperature of decomposition and ii. an increase in char yield compared with the untreated cellulose samples. The indicator for the effectiveness of and inorganic compound as a flame retardant is lower temperature of active pyrolysis and the higher amount of char as observed by mono and diammonium phosphates. An increased amount of char is correlated with reduced amount of flammable tar. Phosphoric acid and phosphate compounds show potential flame retardancy to cellulose backbone by catalyzing the dehydration reactions to produce more char. This reaction pathway is just one of several that are taking place simultaneously, including decarboxylation, condensation and decomposition. It is already proven that the flame-retardants containing nitrogen and phosphorus is highly effective towards decomposition involving cellulose backbone.

Compounds with acidic behavior have prominent effect by reducing the amount of flammable volatiles and as a result, the amount of char is increased. Lewis acids such as zinc (II) chloride found to increase the amount of residual char. Although very hygroscopic, zinc (II) chloride is an effective flame retardant. Mono and diammonium phosphates, which produce phosphoric acid, also reduce the flammable volatiles. Dehydration of glucose units are catalyzed by acidic compounds by the addition of a proton to the hydroxyl oxygen atom to yield unstable carbonium ion, which in turn rearranges and regenerates the proton, thereby propagating the process. The depolymerization of polysaccharide chains is also resulted by the attack from a proton to the glycosidic linkages. The proton forms a conjugate acid with the glycosidic oxygen. The carbon-oxygen bond is cleaved to form an intermediate cyclic carbonium cation, which initiates the addition of a water molecule yielding a stable product and release of the proton.

Fire retardants, which are acidic in nature, may not only catalyze dehydration and depolymerization of cellulose ethers to lesser volatiles yielding more char, but they may also enhance the condensation of the char to result thermally stable cross-linked polycyclic aromatic structures.

Simple ethers of cellulose such as MC and EC undergo two stages of decomposition. HPMC and CMC also exhibit two distinct stages of thermal decomposition. However, HEC shows single major mass loss stage in thermogram. Phenomenological data of thermal decomposition of untreated cellulose ethers are presented in Table-1-5. Thermal stability of cellulose ethers increase in an oxidative atmosphere in the order $\text{HEC} < \text{CMC} < \text{MC} < \text{HPMC} < \text{EC}$. The TG-DTG-DTA profile is shown for MC (Figure-1) and CMC (Figure-2).

The highest char yield of 54.6% denoted for sodium salt of CMC in air and is believed to be the result of combined effect of dehydration, inhibition of depolymerisation and presence of alkali metal ion. HEC also shows high char yield of 32.0% at endset of main stage of decomposition. It is due to the result of enhanced dehydration reaction which increases the thermal stability of HEC against its decomposition and reduces the formation of flammable volatile which result in less loss of carbon from char^{5,6}. This increases the char yield. Based on increase in char yield cellulose ethers follows the order $\text{CMC} < \text{HEC} < \text{HPMC} < \text{MC} < \text{EC}$.

EC gives less char compared to MC. It is because all other compounds except EC has DTG peak temperature shifted to lower values compared to pure microcrystalline cellulose. The DTG peak shifting to lower values indicates the acceleration of onset of weight loss, which obviously increases char yield.

The order parameter of cellulose ethers ranges from 1.2 (CMC) to 2.2 (HEC) for the first decomposition stage. Except for ethyl cellulose all other ethers shows positive values of entropy of activation. Positive values of entropy of activation suggest that the activated complexes in all the cases are less ordered than the respective reactants, and hence, the decomposition reactions are faster than normal. However, for EC, as mentioned earlier, decomposition reactions are retarded, hence show negative value of entropy of activation. The pre-exponential factor is maximum for CMC ($\sim 10^{27}$) while it is minimum for EC ($\sim 10^{11}$). The correlation coefficients are greater than or equal to 0.9957 for cellulose ethers. The activation energies for the main decomposition stage of cellulose ethers follow the order $\text{EC} < \text{HEC} < \text{HPMC} < \text{MC} < \text{CMC}$. Comparison of thermal decomposition characteristics and kinetic parameters (Table-7) shows that the thermal stability and the char yield of cellulose ethers shows a pronounced dependency on substituted groups.

Methyl cellulose and additive doped samples containing methyl cellulose as substrate shows two distinct stages of decomposition except for boric acid as additive. TG-DTG-DTA curves of MC doped with zinc(II) chloride is shown in

Fig.3. Boric acid doped methyl cellulose shows single stage decomposition. The thermal stability of additive doped MC samples increases in the order $MC + ZnCl_2 < MC + (NH_4)_2HPO_4 < MC + CdBr_2 < MC + H_3BO_3 < MC + (NH_4)_2SO_4 \cdot NiSO_4 \cdot 6H_2O < MC < MC + Borax < MC + NaH_2PO_4$

The char yield of samples follows the order (Table-1). $MC + ZnCl_2 < MC + (NH_4)_2HPO_4 < MC + H_3BO_3 < MC + NaH_2PO_4 < MC + Borax < MC < MC + (NH_4)_2SO_4 \cdot NiSO_4 \cdot 6H_2O < MC + CdBr_2$

The highest char yield is obtained at the end set of first decomposition stage of MC with $ZnCl_2$ (50.1%) and $(NH_4)_2HPO_4$ (40.7%). Borax, ammonium nickel (II) sulphate and cadmium (II) bromide have little effect on char production compared with MC. The above said additives are proven flame retardants for MCC, but, found to be ineffective to retard flame spread in MC. For the major mass loss stage, the order parameter ranges from 0.9 to 1.5 for additive-doped samples. The highest values of kinetic parameters ($E=360.8 \text{ kJmol}^{-1}$, $A=3.7 \times 10^{32} \text{ s}^{-1}$, $\Delta S=373.4 \text{ JK}^{-1}\text{mol}^{-1}$) are found for $(NH_4)_2HPO_4$ and lowest values for ammonium nickel(II) sulphate ($E=138.0 \text{ kJmol}^{-1}$, $A=1.8 \times 10^{10} \text{ s}^{-1}$, $\Delta S=-54.2 \text{ JK}^{-1}\text{mol}^{-1}$) for main decomposition stage. The entropy of activation is positive for all decomposition stages except for the first stage involving $(NH_4)_2HPO_4$ as additive and second stage involving $CdBr_2$, NaH_2PO_4 and borax. The kinetic parameters of MC impregnated with additives are depicted in Table-6. The activation energy for the first stage of decomposition of samples involving MC increases in the order $MC + (NH_4)_2SO_4 \cdot NiSO_4 \cdot 6H_2O < MC + Borax < MC + CdBr_2 < MC + ZnCl_2 < MC + NaH_2PO_4 < MC + H_3BO_3 < MC + (NH_4)_2HPO_4$

EC shows two-stage decomposition and the additives such as $CdBr_2$, H_3BO_3 , Borax and $(NH_4)_2HPO_4$ also forces the reaction in to two distinct stages (Table-2). Based on the DTG peak temperature, the thermal stability of samples containing ethyl cellulose increases in the order $EC + H_3BO_3 < EC + ZnCl_2 < EC + (NH_4)_2HPO_4 < EC + CdBr_2 < EC + Borax < EC + (NH_4)_2SO_4 \cdot NiSO_4 \cdot 6H_2O < EC + NaH_2PO_4 < EC$.

The first DTG peak of MC and EC falls at 320°C and 335°C respectively. When $ZnCl_2$ is used as additive both EC and MC shows the first DTG peak at 228°C , but if H_3BO_3 is used for doping, DTG peak values are 312°C and 297°C for MC and EC respectively. Likewise, diammonium hydrogenphosphate shows similar DTG peak values for both alkyl celluloses. In addition, AHP doped ethyl and methyl cellulose exhibits a unique sharp DTG peak above 600°C with corresponding exothermic peaks. These clearly indicate that the substituted groups on glucosan units, irrespective of structural similarities show strong dependency on the nature of additives. The char residue remains at the end set of first stage of decomposition is maximum when $ZnCl_2$ is used as additive where it is 33.4%. Pure EC and EC doped with NaH_2PO_4 and ammonium nickel(II) sulphate shows negative values for entropy of

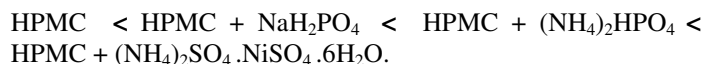
activation. All other main decomposition stages are characterized by positive values of entropy. When EC is used as substrate, maximum values for kinetic parameters ($E=399.1 \text{ kJmol}^{-1}$, $A=3.0 \times 10^{36} \text{ s}^{-1}$, $\Delta S=448.2 \text{ JK}^{-1}\text{mol}^{-1}$) are shown by $(NH_4)_2HPO_4$ and minimum values ($E=126.4 \text{ kJmol}^{-1}$, $A=6.2 \times 10^8 \text{ s}^{-1}$, $\Delta S=-82.6 \text{ JK}^{-1}\text{mol}^{-1}$) by NaH_2PO_4 .

The sample of HEC shows single stage decomposition while in presence of additive; multiple stages are found (Table-3). When H_3BO_3 and NaH_2PO_4 are used as additive, decomposition is completed in three distinct stages and all other additives force the decomposition to complete in two stages. If the thermal stability of HEC is compared with additive impregnated samples, it increases in the order $HEC + ZnCl_2 < HEC + H_3BO_3 < HEC + Borax < HEC < HEC + (NH_4)_2HPO_4 < HEC + NaH_2PO_4 < HEC + CdBr_2 < HEC + (NH_4)_2SO_4 \cdot NiSO_4 \cdot 6H_2O$.

The DTA peaks for all the decomposition stages are found to be exothermic for all samples with HEC. At the end set of first decomposition stage, char yield of 32.0% is observed for HEC. Additives such as NaH_2PO_4 , ammonium nickel(II) sulphate and $(NH_4)_2HPO_4$ produce less residual char compared to HEC. Char yield of various samples follows the order $HEC + H_3BO_3 < HEC + Borax < HEC + ZnCl_2 < HEC + CdBr_2 < HEC + NaH_2PO_4 < HEC + (NH_4)_2SO_4 \cdot NiSO_4 \cdot 6H_2O < HEC + (NH_4)_2HPO_4$.

Entropy of activation for all samples containing HEC is positive except for the binary mixture containing borax. In the series using HEC, the values of kinetic parameters are minimum for the sample using borax as additive ($E=157.9 \text{ kJmol}^{-1}$, $A=2.5 \times 10^{12} \text{ s}^{-1}$, $\Delta S=-12.7 \text{ JK}^{-1}\text{mol}^{-1}$). If the sample shows more than a single stage of decomposition, then one with minimum activation energy will be of first stage. When the first stage of decomposition are compared, cadmium (II) bromide impart highest values for the kinetic parameters ($E=215.3 \text{ kJmol}^{-1}$, $A=8.4 \times 10^{17} \text{ s}^{-1}$, $\Delta S=92.9 \text{ JK}^{-1}\text{mol}^{-1}$). Among the seventeen decomposition process in this series involving HEC, the activation energy is maximum for the third decomposition stage involving NaH_2PO_4 (483.0 kJmol^{-1}) while pre-exponential factor and entropy of activation are maximum for the final decomposition stage using boric acid as additive.

Except borax, all other additives along with HPMC show two distinct stages of decomposition (Table-4). After the main decomposition stage of HPMC, the residue remains is 25.6%. When zinc (II) chloride is used as additive, the DTG peak temperature is shifted to lower value by 77°C . The endothermic region observed for this sample is due to the strong dehydration effected by the Lewis acid and char yield increases to 37.8%. The major decomposition reactions can be noticeably accelerated by the additives such as zinc (II) chloride, boric acid and cadmium(II) bromide. The thermal stability of samples using HPMC as substrate increases in the order $HPMC + ZnCl_2 < HPMC + H_3BO_3 < HPMC + CdBr_2 < HPMC + Borax <$



The sample of HPMC doped with sodium hydrogenphosphate shows the highest values for kinetic parameters for the major mass loss stage ($E=267.7 \text{ kJmol}^{-1}$, $A=1.1 \times 10^{21} \text{ s}^{-1}$, $\Delta S = 152.4 \text{ JK}^{-1} \text{ mol}^{-1}$) and cadmium (II) bromide gives the minimum values among the series ($E=182.1 \text{ kJmol}^{-1}$, $A=1.3 \times 10^{14} \text{ s}^{-1}$, $\Delta S = 19.6 \text{ JK}^{-1} \text{ mol}^{-1}$). For the second stage of decomposition, highest values for kinetic parameters are shown by ammonium nickel(II) sulphate. Entropy of activation is positive for all decomposition stages involving HPMC.

Phenomenological data for the thermal decomposition of CMC and CMC impregnated with flame retardant additives shows that all samples complete decomposition in two stages and all the sixteen stages are exothermic in nature (Table-5).

It is also found that additives slightly increases the thermal stability of CMC except zinc (II) chloride. Among the five cellulose ethers discussed here, CMC produces maximum amount of stable residual char after the end set of main decomposition stage. It is evident from the sharp DTG peaks at higher temperature, which is due to the oxidative gasification of stable scission compounds produced at relatively lower temperature. Zinc (II) chloride act as a retardant for the oxidation in final stage and shifts the DTG peak temperature to 633°C in comparison with CMC (609°C). Maximum thermal stability is exhibited by boric acid doped CMC with maximum char yield (60.5%). Char yield of various samples increases the order $\text{CMC} + \text{H}_3\text{BO}_3 < \text{CMC} + \text{CdBr}_2 < \text{CMC} + \text{Borax} < \text{CMC} + (\text{NH}_4)_2\text{HPO}_4 < \text{CMC} + \text{ZnCl}_2 < \text{CMC} < \text{CMC} + \text{NaH}_2\text{PO}_4 < \text{CMC} + (\text{NH}_4)_2\text{SO}_4 \cdot \text{NiSO}_4 \cdot 6\text{H}_2\text{O}$.

The kinetic parameters of second stage decomposition for the samples containing CMC are much higher than that obtained for the first stage. When NaH_2PO_4 is used as additive, it gives the maximum values for the kinetic parameters such as $E=387.4 \text{ kJmol}^{-1}$, $A=1.8 \times 10^{34} \text{ s}^{-1}$, $\Delta S = 405.4 \text{ JK}^{-1} \text{ mol}^{-1}$ for the major mass loss stage. Maximum value of E implies that with comparatively higher activation energy, once activated, sample undergoes very rapid decomposition giving high gas evolution and char residue was decreased. The minimum values of kinetic parameters are exhibited by boric acid with order parameter 1.7 for the first decomposition stage ($E=237.8 \text{ kJmol}^{-1}$, $A=9.2 \times 10^{19} \text{ s}^{-1}$, $\Delta S = 131.9 \text{ JK}^{-1} \text{ mol}^{-1}$) which produces higher char residue. The correlation coefficients are closer to unity for all samples. ΔS for all the decomposition stages are found to be positive indicating a less ordered activated species in these thermal activation processes.

The mechanisms of thermal decomposition reactions of all the samples have also been elucidated, and the reactions follow the Mampel equation indicating the mechanism of random nucleation with one nucleus on each particle⁴.

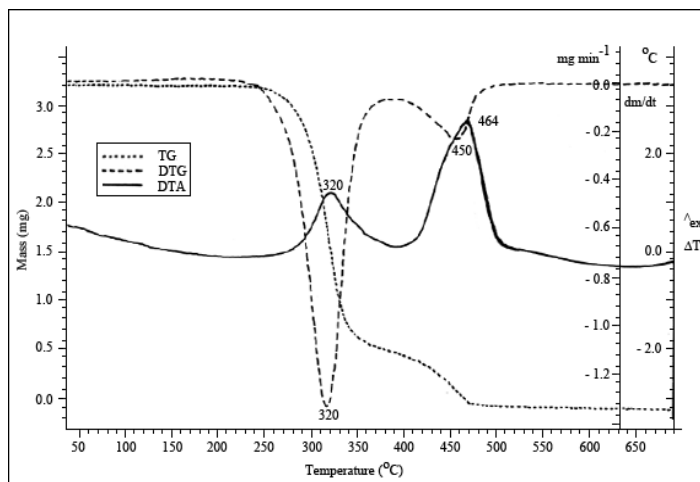


Figure-1
TG-DTG-DTA curves of MC

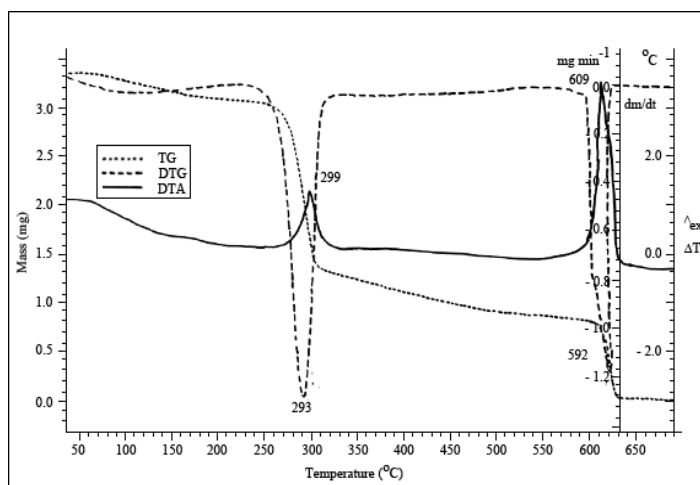


Figure-2
TG-DTG-DTA curves of CMC

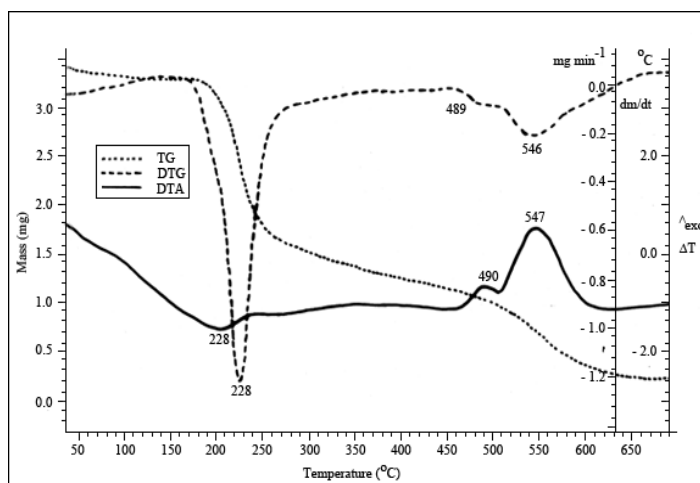


Figure-3
TG-DTG-DTA curves of MC doped with zinc (II) chloride

Table-1
Thermal decomposition data of MC with FR additives

Sample	Plateau in TG	Stage	DTG peak T	DTA peak T	Residue (%)
MC	Up to 250 After 480	I	320	320	24.5
		II	450	464	3.0
MC + ZnCl ₂	Up to 180 After 650	I	228	240	50.1
		II	546	547	9.0
MC + CdBr ₂	Up to 250 After 590	I	311	321	23.0
		II	449	450	12.0
MC + H ₃ BO ₃	Up to 280 After 700	I	312	318	33.4
MC+ Borax	Up to 240 After 500	I	324	322	24.7
		II	481	483	7.0
MC + AHP	Up to 250 After 700	I	278	284	40.7
		II	615	609	12.3
MC + SHP	Up to 280 After 500	I	328	326	29.4
		II	487	487	10.2
MC+ANS	Up to 210 After 500	I	317	289	23.4
		II	475	478	3.6

Table-2
Thermal decomposition data of EC with FR additives

Sample	Plateau in TG	Stage	DTG peak T	DTA peak T	Residue (%)
EC	Up to 210 After 440	I	335	354	12.7
		II	423	428	2.9
EC + ZnCl ₂	Up to 160 After 700	I	228	226	33.4
EC + CdBr ₂	Up to 190 After 430	I	321	327	12.7
		II	386	384	3.0
EC + H ₃ BO ₃	Up to 200 After 700	I	212	212	84.3
		II	297	298	25.2
EC + Borax	Up to 190 After 490	I	330	345	20.6
		II	448	457	6.7
EC + AHP	Up to 200 After 650	I	279	280	30.3
		II	625	628	3.4
EC+SHP	Up to 270 After 650	I	335	343	14.5
EC +ANS	Up to 200 After 500	I	332	334	16.2

Table-3
Thermal decomposition data of HEC with FR additives

Sample	Plateau in TG	Stage	DTG peak T	DTA peak T	Residue (%)
HEC	Up to 220 After 500	I	290	296	32.0
HEC+ ZnCl ₂	Up to 150 After 560	I	280	276	35.6
		II	522	522	6.1
HEC+ CdBr ₂	Up to 220 After 560	I	294	298	33.5
		II	506	500	5.9
HEC+H ₃ BO ₃	Up to 210 After 550	I	288	293	4.1
		II	406	410	29.2
		III	525	526	9.2
HEC+ Borax	Up to 230 After 670	I	289	297	43.8
		II	412	418	22.6
HEC+ AHP	Up to 150 After 620	I	291	299	29.6
		II	488	487	12.5
HEC+SHP	Up to 190 After 660	I	293	299	30.5
		II	483	480	21.8
		III	630	632	7.5
HEC +ANS	Up to 230	I	298	303	30.3
	After 610	II	503	506	11.7

Table-4
Thermal decomposition data of HPMC with FR additives

Sample	Plateau in TG	Stage	DTG peak T	DTA peak T	Residue (%)
HPMC	Up to 240 After 530	I	326	324	25.6
		II	458	461	9.1
HPMC+ ZnCl ₂	Up to 200 After 550	I	249	243	37.8
		II	526	531	5.7
HPMC+ CdBr ₂	Up to 230 After 540	I	319	323	29.3
		II	528	528	5.9
HPMC+H ₃ BO ₃	Up to 250 After 700	I	318	321	30.9
		II	531	531	6.3
HPMC+ Borax	Up to 220 After 570	I	324	325	23.8
HPMC + AHP	Up to 230 After 650	I	328	329	22.9
		II	477	485	7.8
HPMC + SHP	Up to 220 After 490	I	326	322	26.1
		II	462	465	5.7
HPMC +ANS	Up to 220 After 480	I	330	331	23.8
		II	476	481	6.7

Table-5
Thermal decomposition data of CMC with FR additives

Sample	Plateau in TG	Stage	DTG peak T	DTA peak T	Residue (%)
CMC	Up to 80 After 610	I	293	299	54.6
		II	592	609	24.0
CMC + ZnCl ₂	Up to 80 After 700	I	290	297	56.6
		II	633	638	29.4
CMC + CdBr ₂	Up to 240 After 590	I	293	298	57.8
		II	586	582	25.0
CMC +H ₃ BO ₃	Up to 80 After 700	I	299	304	60.5
		II	630	632	22.5
CMC + Borax	Up to 80 After 650	I	292	298	57.6
		II	605	613	27.7
CMC + AHP	Up to 80 After 610	I	294	300	57.2
		II	596	602	27.2
CMC + SHP	Up to 80 After 640	I	294	297	54.5
		II	605	607	24.3
CMC +ANS	Up to 210 After 500	I	293	300	54.0
		II	606	605	24.0

Table-6
Comparison of kineticdata for thermal decomposition of cellulose ethers

Sample	Stage	Method/ Mechanism	E (kJmol ⁻¹)	A (s ⁻¹)	ΔS (JK ⁻¹ mol ⁻¹)	r
MC	I	Coats-Redfern; n=2.1	263.6	5.6x10 ²¹	165.7	0.9988
		Random nucleation	208.7	2.7x10 ¹⁶	64.0	0.9966
	II	Coats-Redfern; n=1.5	269.4	3.5x10 ¹⁷	83.6	0.9974
		Random nucleation	237.8	1.4x10 ¹⁵	37.6	0.9957
EC	I	Coats-Redfern; n=1.5	150.5	1.5x10 ¹¹	-37.1	0.9976
		Random nucleation	135.5	4.9x10 ⁹	-65.4	0.9969
	II	Coats-Redfern; n=1.2	261.9	7.6x10 ¹⁷	90.3	0.9997
		Random nucleation	246.1	3.5x10 ¹⁶	64.8	0.9995
HEC	I	Coats-Redfern; n=2.2	174.6	1.1x10 ¹⁴	18.9	0.9957
		Random nucleation	123.1	7.3x10 ⁸	-80.5	0.9710
HPMC	I	Coats-Redfern; n=1.5	227.8	1.1x10 ¹⁸	94.5	0.9998
		Random nucleation	190.4	3.0x10 ¹⁴	26.5	0.9965
	II	Coats-Redfern; n=1.5	409.0	4.2x10 ²⁷	276.5	0.9989
		Random nucleation	364.2	1.7x10 ²⁴	211.5	0.9979
CMC	I	Coats-Redfern; n=1.2	320.1	8.9x10 ²⁷	284.9	0.9997
		Random nucleation	300.1	9.4x10 ²⁵	247.0.	0.9995

Table-7
Kinetic Parameters for the thermal decomposition of MC with FR additives

Sample	Stage	Method/ Mechanism	E (kJmol ⁻¹)	A (s ⁻¹)	ΔS (JK ⁻¹ mol ⁻¹)	r
MC	I	Coats-Redfern; n=2.1	263.6	5.6x10 ²¹	165.7	0.9988
		Random nucleation	208.7	2.7x10 ¹⁶	64.0	0.9966
	II	Coats-Redfern; n=1.5	269.4	3.5x10 ¹⁷	83.6	0.9974
		Random nucleation	237.8	1.4x10 ¹⁵	37.6	0.9957
MC + ZnCl ₂	I	Coats-Redfern; n=1.5	219.5	1.3x10 ²¹	154.7	0.9999
		Random nucleation	187.9	1.4x10 ¹⁷	87.8	0.9984
	II	Coats-Redfern; n=2.0	339.2	2.4x10 ¹⁹	117.7	0.9993
		Random nucleation	271.0	6.5x10 ¹⁴	30.2	0.9907
MC + CdBr ₂	I	Coats-Redfern; n=1.3	208.4	4.2x10 ¹⁶	67.7	0.9998
		Random nucleation	182.9	1.6x10 ¹⁴	21.4	0.9972
	II	Coats-Redfern; n=1.7	181.2	8.8x10 ¹⁰	-42.8	0.9975
		Random nucleation	142.2	6.9x10 ⁷	-102.2	0.9915
MC + H ₃ BO ₃	I	Coats-Redfern; n=1.0	271.0	1.0x10 ²⁴	209.5	0.9993
		Random nucleation	271.0	1.0x10 ²⁴	209.5	0.9993
MC+ Borax	I	Coats-Redfern; n=1.2	202.0	7.2x10 ¹⁵	52.8	0.9988
		Random nucleation	188.7	4.1x10 ¹⁴	29.0	0.9980
	II	Coats-Redfern; n=1.1	184.6	7.3x10 ¹⁰	-44.6	0.9902
		Random nucleation	179.6	2.9x10 ¹⁰	-52.3	0.9899
MC + AHP	I	Coats-Redfern; n=1.5	360.8	3.7x10 ³²	373.4	0.9999
		Random nucleation	303.5	7.7x10 ²⁶	264.7	0.9967
MC + SHP	I	Coats-Redfern; n=1.2	227.7	9.8x10 ¹⁷	93.7	0.9989
		Random nucleation	213.7	5.1x10 ¹⁶	69.0	0.9985
	II	Coats-Redfern; n=0.9	185.4	6.0x10 ¹⁰	-46.3	0.9964
		Random nucleation	191.2	1.7x10 ¹¹	-37.8	0.9965
MC+ANS	I	Coats-Redfern; n=0.9	138.0	1.8x10 ¹⁰	-54.2	0.9994
		Random nucleation	142.2	4.6x10 ¹⁰	-46.4	0.9994
	II	Coats-Redfern; n=1.1	236.9	3.8x10 ¹⁴	26.5	0.9980
		Random nucleation	222.0	2.9x10 ¹³	5.2	0.9976

Conclusion

This investigation establishes the stability and solid state decomposition kinetics of five cellulose ethers and their 5% (w/w) additive doped mixtures. The thermal stability and the char yield of cellulose ethers and additive doped samples exhibits a strong dependency on substituted groups on cellulose back bone and the nature in which the additive react with it. The thermal decomposition reactions of all the samples follow the Mampel equation, and hence, these reactions follow random nucleation with one nucleus on each particle. It is evident from the decomposition characteristics that cellulose ethers can be fireproofed with the retardants used for flame proofing cellulose, but not all, with the same efficiency. It is crucial to have a detailed observation in choosing suitable additive for particular cellulose ether to exhibit maximum flame retardancy.

References

1. Cathleen Baker (1982). Methylcellulose & Sodium Carboxymethylcellulose: Uses in Paper Conservation. The Book and Paper Group Annual, 1.
2. Xin-Gui Li, Mei-Rong Huang and He Bai (1999). Thermal decomposition of cellulose ethers. *Journal of Applied Polymer Science*, 73, 2927-2936.
3. Coats A.W. and Redfern (1964). Kinetic parameters from thermogravimetric data. 201, 68-69
4. Satava V. (1971). Mechanism and kinetics from non-isothermal TG traces. *Thermochim. Acta.*, 2, 423-428.
5. Brown A.L., Dayton D.C. and Daily J.W. (2001). A study of cellulose pyrolysis chemistry and global kinetics at high heating rates. *Energy & Fuels.*, 15, 1286-1294.
6. Browne F. L. (1958). Theories of the combustion of wood and its control., U.S Forest Products Laboratory Report, No. 2136., Madison., Wisconsin.